High-pressure structural properties of tetramethylsilane*

Zhen-Xing Qin(秦振兴)[1,2] and Xiao-Jia Chen(陈晓嘉)[3,†]

[1] Department of Physics, Taiyuan University of Science and Technology, Taiyuan 030024, China
[2] Department of Physics, South China University of Technology, Guangzhou 510640, China
[3] Center for High Pressure Science and Technology Advanced Research, Shanghai 201203, China

(Received 1 July 2015; revised manuscript received 29 October 2015; published online 10 January 2016)

High-pressure structural properties of tetramethylsilane are investigated by synchrotron powder x-ray diffraction at pressures up to 31.1 GPa and room temperature. A phase with the space group of *Pnma* is found to appear at 4.2 GPa. Upon compression, the compound transforms to two following phases: the phase with space groups of $P2_1/c$ at 9.9 GPa and the phase with $P2/m$ at 18.2 GPa successively via a transitional phase. The unique structural character of $P2_1/c$ supports the phase stability of tetramethylsilane without possible decomposition upon heavy compression. The appearance of the $P2/m$ phase suggests the possible realization of metallization for this material at higher pressure.

Keywords: hydrogen-rich compounds, structural properties, high pressure

PACS: 61.50.–f, 64.70.K–, 07.85.Qe **DOI:** 10.1088/1674-1056/25/2/026104

1. Introduction

As an important challenge in modern physics and astrophysics, the metallization of hydrogen has long been a major driving force in high-pressure science and technology development,[1] which originates from the possible superconductivity with high T_c($>$ 200 K) under sufficiently strong compression.[2,3] Recently, several independent measurements indicate that metallic hydrogen has not been reached yet even at 360 GPa,[4,5] whereas much higher pressures (e.g., $>$ 400 GPa) are thought to be needed for metallization,[6] which currently are a great challenge for hydrogen with high-pressure techniques. In 2004, Ashcroft already with great interest suggested that hydrogen-dominant hydrides could also be high-temperature superconductors in monatomic and molecular phases, providing an alternative way to achieve the metallic hydrogen. By this argument, such covalent hydrides could exhibit metallization at significantly reduced pressures compared with pure hydrogen due to chemical precompression.[7] The recent breakthrough in the discovery of superconductivity above record high 190 K in H–S compound[8] offers convincing evidence for this idea. Group IVa hydrides were specifically suggested as potential candidates for this material and many experimental and theoretical efforts are currently underway to investigate this prediction, such as SiH_4,[9–18] GeH_4,[19–23] SnH_4,[24–27] and PbH_4.[28] However, very recent experiments show the possible decomposition of SiH_4 under irradiations from x-ray and lasers,[29,30] which results in a loss of superiority for these compounds to further investigate the metallization of bulk hydrogen. For achieving the metallic hydrogen at "low" pressure, it is extremely urgent to search other hydrogen-rich compounds on the group IVa hydrides.

Tetramethylsilane (TMS), $Si(CH_3)_4$, has spurred tremendous interest in the spectrum due to its highly symmetrical characters.[31–36] In the molecular structure in Fig. 1(a), the Si element is tetrahedrally coordinated by methyl groups (–CH_3), making the molecule with the T_d symmetry.[34,36] Study on TMS under low temperature condition suggested that the CH_3 groups play an central role in understanding the structural transformation and the CH_3 groups become non-equivalent due to intermolecular interactions.[37] Upon compression, TMS becomes a single crystal with cubic structure only at 0.58 GPa, accompanied with the CH_3 groups to display different rotational angles (Fig. 1(b)).[38] Besides new phase transitions at higher pressures, our recent work by Raman spectrum revealed that TMS does not decompose at pressures up to 142 GPa,[39] although the metallization has not been reached yet. However, new Raman modes, appearing at around 100 GPa,[39] underwent a dramatic softening and characterized TMS as semi-metallic state possibly as in the case of hydrogen at high pressures.[4] This suggests that the TMS, maybe, will be an ideal material to achieve metalization in hydrogen-rich complex on the basis of the static high-pressure technology currently.

On the basis of the global minimization of the lattice energy, several competitive crystal structures have been proposed for the phases of TMS in recent computational studies,[37] while there are only a few experimental data for its molecular and crystal structures even at lower pressures.[38,40] Such

*Project supported by the Cultivation Fund of the Key Scientific and Technical Innovation Project from Ministry of Education of China (Grant No. 708070), the Fundamental Research Funds for the Central Universities, South China University of Technology (Grant No. 2014ZZ0069), the National Natural Science Foundation of China (Grant No. 51502189), and the Doctoral Project of Taiyuan University of Science and Technology, China (Grant No. 20132010).

†Corresponding author. E-mail: xjchen@hpstar.ac.cn

information is important for understanding the evolution in the electronic structure leading to metallization. In this paper, we present a high-pressure study of TMS by synchrotron powder x-ray diffraction (XRD) at up to 31.1 GPa. We observe a similar process of phase transitions although it shows slight hysteresis compared with the results from Raman spectrum. TMS underwent $Pnma \rightarrow P2_1/c \rightarrow P2/m$ structural transitions via $Pa\bar{3}$ symmetrial crystal at 0.58 GPa,[38] which will be illustrated in Section 3 in detail.

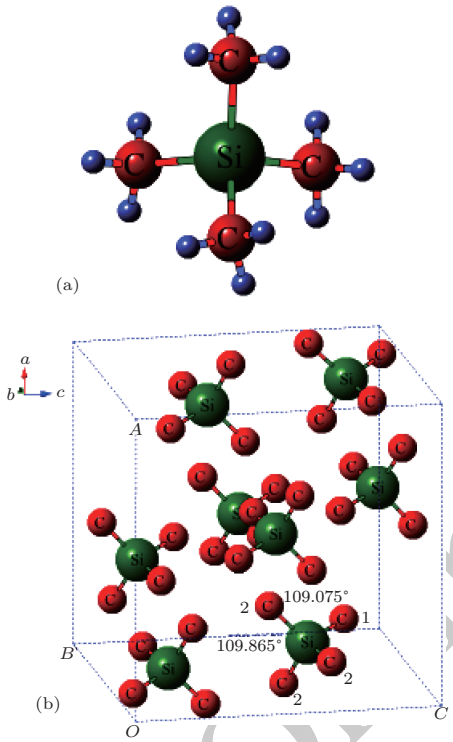

Fig. 1. (color online) (a) Configurations of TMS with respect to ideally tetrahedral $T_d(\bar{4}3m)$ symmetry; (b) autostereogram of the molecular arrangement in the prassure-induced $Pa\bar{3}$ symmetrial crystal of TMS with different rotational angles of the CH_3 groups (except for H atoms).

2. Experimental details

TMS (m.p. 178 K, b.p. 299 K) as transparency liquid with 99.9% purity was purchased from Alfa-Aesar and used without further purification. The high-pressure experiments for TMS were carried out by using Diamond anvil cell (DAC) with beveled anvils and the culets of 300 μs. A hole of ∼ 100 μs in diameter, drilled in a preindented tungsten gasket, served as the sample chamber. To avoid volatilizing, the bottom of DAC was put into ice-water mixture half an hour before loading the sample. Liquid TMS was loaded into the chamber of DAC with a syringe. Because of liquid sample, no pressure medium was used and ruby grains had been placed previously as pressure marker. Considering the volatilizing of samples, pressure was increased to 0.6 GPa after loading well the samples. Synchrotron radiation measurements were performed at the X17C beamline of National Synchrotron Light Source at Brookhaven National Laboratory via angle-dispersive diffraction techniques by using monochromatic radiation $\lambda = 0.3989$ Å. The sample-to-detector distance and the image plate orientation angles were calibrated by using CeO_2 standard. The two-dimensional (2D) diffraction images were converted to the plots of 2θ versus intensity by the FIT2D software.

3. Results and discussion

Synchrotron powder x-ray diffraction measurements on TMS are performed to determine detailed structural information for the possible phases under pressure. Figure 2 shows the x-ray diffraction patterns of TMS at pressure up to 31.1 GPa. All the Bragg peaks shift towards larger angles, showing the shrinkage of the TMS lattice. At 4.2 GPa, x-ray diffraction pattern of TMS reveals a strong preferred orientation from the peak at 5.5°–6.0°, which possibly results from the recrystallization of TMS. Until 9.9 GPa, all peaks become smooth accompanied by some peaks vanishing and new peaks appearing in a pressure range of 6.5 GPa–8.6 GPa, suggesting a new phase transition taking place. A similar case has been observed in recent work[39,40] that a new phase transition appeared at 9.0 GPa by the analysis of Raman spectrum. Upon further compression to 18.2 GPa, the XRD pattern of the sample exhibits the whole changes, especially the peaks in the region of low angles, indicating that another structural transformation appears. The new phase shows slight hysteresis compared with the recent experimental results of the phase transition of TMS at 16.0 GPa.[39] Continuing the compression to 31.1 GPa, no change is observed from the XRD patterns, which coincides with the results of Raman spectral experiments in our recent work.[39]

To investigate the crystal structure of each phase, the diffraction patterns obtained at selected pressures are indexed using Dicvo104 and refined using the Le Bail method with GSAS software.[41] For TMS, it is reported that TMS crystallizes into cubic structure with the space group $Pa\bar{3}$,[38] which is marked as phase II via liquid phase (phase I), with being compressed to only 0.58 GPa. Based on the analysis of high-pressure Raman spectrum,[39] cubic structure at least should be maintained with compression to 9.0 GPa. However, it is difficult to fit the XRD pattern at 4.2 GPa using the space group $Pa\bar{3}$ with lattice parameter $a = 10.7328$ Å. Indexing yields a reasonable solution, which leads to an orthorhombic cell (space group *Pnma*) at this pressure.[39] Additionally, a study of possible crystal structures of TMS is performed by global lattice-energy minimization using force-field methods.[37] The results indicate that the *Pnma* space group is

the second low-energy structure for TMS.[37] The phase is fitted with the space group of *Pnma* and the measured and fitted data are shown in Fig. 3(a). As can be seen, the diffraction peaks of TMS at 4.2 GPa are fitted well within the indexed structure, marked as phase III. For substances with "normal" melting curve, cooling down and compression in a small P–T region often produce equivalent solid phases.[42] It so happens that low-temperature TMS would undergo $\alpha \rightarrow \beta \rightarrow \gamma$ phase transitions (α phase exists from the melting point down to 159 K; with further cooling β phase appears and becomes stable to 20 K; when the sample is subsequently heated from 20 K to 118 K γ phase occurs.[43]) and only γ phase is stable when heated to 118 K,[44] which should be consistent with low-temperature crystallization to transform into a single crystal (space group *Pnma*) with lattice parameters of $a = 13.131(3)$ Å, $b = 8.198(3)$ Å, and $c = 6.3290(10)$ Å.[37] Compared with our results of $a = 13.0479(3)$ Å, $b = 8.4526(4)$ Å, and $c = 6.2857(9)$ Å at 4.2 GPa, however, axis b is stretched relatively. A plausible cause for the abnormity is nonhydrostatic situation of crystallized TMS at high pressures, which leads to the lattice distortion.

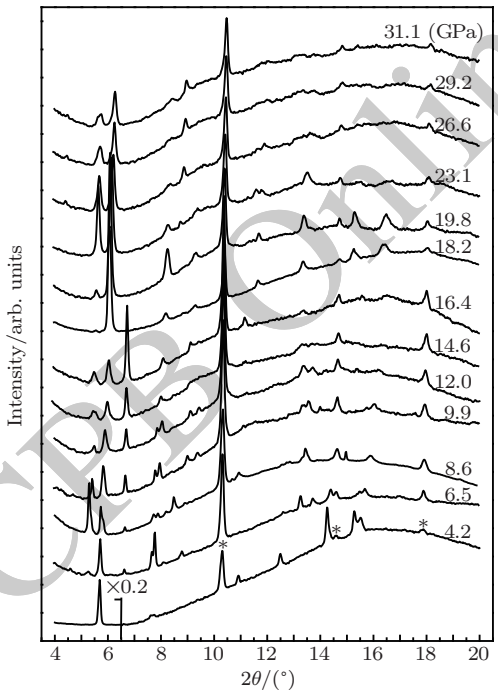

Fig. 2. Synchrotron radiation x-ray ($\lambda = 0.3989$ Å) diffraction patterns of TMS during the pressurization from ambient pressure to 31.1 GPa. Red asterisks marked indicate the signals from the gasket material tungsten. The intensity of first peak is reduced to 1/5 at 4.2 GPa due to strong preferred orientation of (211) in *Pnma* phase.

For phase IV of TMS at 9.9 GPa, all peaks from the XRD pattern are indexed mainly to the monoclinic system. However, it is difficult to determine the space group for this new phase, whereas $P2_1/c$ is a candidate because tetrahalides of the group IVa elements, MX_4 (M = Si, Ge, Sn; X = Cl, Br) with halogen atoms each have a comparable size to a methyl group crystallized in $P2_1/c$.[45–50] Considering the Raman results that CH_3 groups are locked in position and the whole groups move like one atom,[39] the $P2_1/c$ space group will be the most reasonable solution to the structure of TMS at phase IV. In addition, the $P2_1/c$ space group is also predicted as the third best structure of TMS energetically and appears repeatedly with increasing the energy of crystal structure.[37] Figure 3(c) shows the results of fitting the pattern of TMS at 9.9 GPa by the space group of $P2_1/c$. In view of the lattice parameters of MX_4 at low temperature (for $SiCl_4$,[45] $a = 9.6084$ Å, $b = 6.3562$ Å, $c = 7.6724$ Å, and $\beta = 102.909°$; for $SiBr_4$,[50] $a = 10.1319$ Å, $b = 6.7002$ Å, $c = 10.2389$ Å, and $\beta = 102.661°$), the lattice parameters of $a = 8.5412(6)$ Å, $b = 8.7889(2)$ Å, $c = 8.3227(4)$ Å, and $\beta = 85°$ are debatable. Axis b is stretched more dramatically, suggesting enhancive lattice distortion in nonhydrostatic situation of crystallized TMS with increasing pressure. In the pressure range of 6.5 GPa–8.6 GPa, phase III coexists with phase IV and the pattern at 6.5 GPa is fitted with both lattice parameters of the phases in Fig. 3(b).

There is no information about crystal structure available at the highest-pressure phase (phase V) of TMS in current work. The diffraction patterns yield several orthorhombic and monoclinic systems at 19.8 GPa with reasonable lattice parameters. According to the study of high-pressure Raman spectrum,[39] phase V should possess lower symmetry because the number of Raman bands greatly increases in the phase,[51] thus the orthorhombic systems have been ruled out. Furthermore, it is quite interesting that all monoclinic cells are characterized by different lattice parameters and the same space group $P2/m$ at this pressure. It might be the most reasonable of the lattice parameters $a = 8.2042$ Å, $b = 3.7287$ Å, $c = 2.4630$ Å, and $\beta = 97.714°$ with a volume of 74.66 Å^3 because of remarkable value of the figures of merit (M, F) at this pressure. Figure 3(d) shows the measured and fitted patterns of TMS at 19.8 GPa. All diffraction patterns at up to 31.1 GPa could be fitted with this cell, suggesting that the phase remains stable until 31.1 GPa.

The R values are $R_p = 0.2\%$, $R_{wp} = 0.4\%$ for the fitting at 4.2 GPa, $R_{p=0.1}\%$, $R_{wp=0.3}\%$ at 6.5 GPa, $R_p = 0.3\%$, $R_{wp} = 0.4\%$ for the fitting at 9.9 GPa, and $R_p = 0.4\%$, $R_{wp} = 0.5\%$ at 19.8 GPa.

$$R_p = \frac{\sum \frac{|I_o - I_c| \cdot |I_o - I_b|}{I_o}}{\sum |I_o - I_c|},$$

$$R_{wp} = \sqrt{\frac{\sum w((I_o - I_c)(I_o - I_b)/I_o)^2}{\sum w(I_o - I_b)^2}},$$

where $\omega = 1/\sigma^2$ is the statistical weight of the i-th profile observation which is the inverse of the variance of the i-th observation.I_o and I_c are observed and calculated intensities, I_b is the background contribution to the profile in Ref. [63].

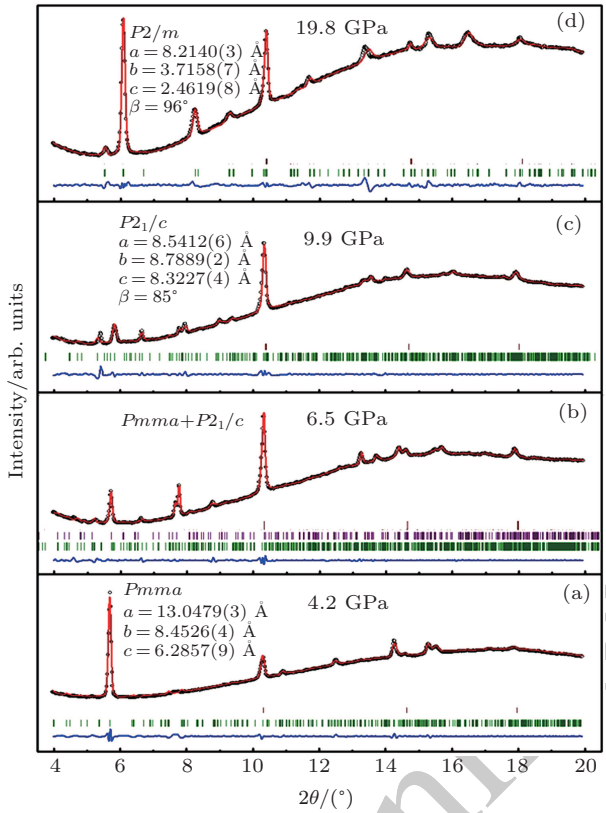

Fig. 3. (color online) X-ray powder diffraction patterns of liquid TMS at pressures of (a) 4.2, (b) 6.5, (c) 9.9, and (d) 19.8 GPa, respectively. The refined lattice parameters for the corresponding space groups are given, respectively. The open circles represent the measured intensities and the red lines represent the results of profile refinements by the best LeBail-fit with each space group. The positions of the Bragg reflections are marked by vertical lines *Pnma* is shown as green and $P2_1/c$ is shown as purple in panel (b) and the difference profiles are shown at the bottoms (blue lines).

Although the use of the Le Bail method can give reasonable space groups and yields accurate lattice parameters of the structures, this method has not provided any information about the internal coordinates. Since the texture of the sample combined with the extraordinarily large hydrogen content presents limitation to meaningful Rietveld structural refinements, as a substitution, we compare the crystal characteristic of TMS at phase IV with that of the typical hydrogen-rich compound SiH_4. The reason is that the structure $P2_1/c$ is the last one for SiH_4 existing before becoming partial decomposition and amorphization or polymerization upon compression despite it is still an insulating molecular solid,[30] which is helpful for us to understand the procedure of structural change on TMS.

For SiH_4 as shown in Table 1, the phase V stable above 10 GPa is reported to possess an $SnBr_4$-type structure (space group $P2_1/c$) in Ref. [30] while the crystal structures of low-pressure phases are as yet unknown. Other tetrahalidies with the $P2_1/c$ structures are also listed in Table 1, it is found from the first four compounds that the ratios of lattice parameter b/a and c/a, are close to each other, and values of angle β keep the same nearly. According to the pressure-induced phase transition analysis by Raman spectrum,[39] CH_3 groups of TMS in phase IV are locked in position and the whole groups move like one atom, which provides a possibility for the phase IV of TMS to reconstruct own molecules like SiH_4, $SnBr_4$, $SiCl_4$, and $SiBr_4$ mentioned above, and $P2_1/c$ symmetry is selected first to fit the pattern in phase IV in this end. However, the corresponding result shows inconsistency among the lattice parameters b/a, c/a, and angle β, which will happen if $P2_1/c$ symmetrical $Ge(CH_3)_4$ (TMGe) appears when compression almost possesses the same lattice parameters as TMS (Table 1).[52] Considering the application of external condition, nonhydrostatic situation of crystallized TMS could be a reasonable explanation for the abnormity, which leads to the lattice distortion compared with $SnBr_4$, $SiCl_4$, and $SiBr_4$ to undergo the structural change depending on temperature.[45,50,53] Whereas the SiH_4 under applied pressure is still kept as an excellent crystal with space group $P2_1/c$ as $SnBr_4$, $SiCl_4$, and $SiBr_4$ behave, suggesting that different pressure activities exist in both $Si(CH_3)_4$ compound and $Ge(Ch_3)_4$ compound. It is worth mentioning that crystal structure of the $P2_1/c$ is the last one for SiH_4 under pressure.[30] Further compression beyond 50 GPa, undetectable x-ray diffractions in some sample regions of SiH_4 suggest the loss of crystallinity, which is consistent with the previous claim of the pressure-induced amorphization.[18] The loss of crystallinity with partial decomposition and amorphization due to the applied pressure has also been reported previously for solids containing relevant tetraheddral molecules like $SnBr_4$, SnI_4, and GeI_4,[54–57] of which similar compounds are SiCl4 and $SiBr_4$ although it is uncertain whether these solids are confirmed to have the $P2_1/c$ symmetrical structure s before amorphization upon compression, since poor information about pressure-induced crystal structural changes was reported for these solids.[55,56,58–60] However, TMS continues to undergo a phase transition to $P2/m$ space group via $P2_1/c$ space group instead of the appearing of pressure-induced decomposition or amorphization. Such a unique $P2_1/c$ structure of TMS must be a cause of undergoing the phase transitions metioned above instead of pressure-induced decomposition or amorphization under applied pressure.

Table 1. Structural characteristics of TMS phase IV compared with those of tetrahalidies having the $SnBr_4$-type structure.

Phase	P,T	Space group	a/Å	b/Å	c/Å	β/(°)	b/a	c/a	Ref.
$SnBr_4$	293 K	$P2_1/c$	10.59(3)	7.10(2)	10.66(3)	103.6(2)	0.670	1.007	53
$SiCl_4$	163 K		9.608(4)	6.356(2)	9.672(4)	102.91	0.661	1.007	45
$SiBr_4$	168 K		10.1319	6.7002	10.2389	102.661	0.661	1.011	50
SiH_4(V)	11.3 GPa, 300 K		6.122(1)	4.072(2)	6.161(1)	104.36(1)	0.661	1.006	12
TMGe(III)	14.5 GPa, 300 K		6.7020(1)	9.4397(8)	6.5710(4)	89	1.408	0.980	52
TMS(IV)	9.9 GPa, 300 K		8.5412(6)	8.7889(2)	8.3227(4)	85	1.029	0.974	this work

Recently, our work on the structure of $Sn(CH_3)_4$ (TMT) by synchrotron x-ray diffraction measurement has shown to crystallize at 12.5 GPa into space group $P2/m$, which yields lattice parameters of $a = 11.8438$ Å, $b = 6.3417$ Å, $c = 2.9825$ Å, and $\beta = 94°$ ($Z = 2$).[61] TMS also confirms the space group $P2/m$ with the lattice parameters of $a = 8.2140$ Å, $b = 3.7158$Å, $c = 2.4619$ Å, and $\beta = 96°$ ($Z = 2$) at phase V via $P2_1/c$ space group upon compression. For the optimal calcuation on $P2/m$ structure of TMT, the results show the metallic character with large dispersion bands crossing the Fermi level although our optical observations seemingly do not support the metallization in TMT,[61] which could be a indication to undergo a metallic state for TMS and TMT soon with increasing pressure. Excitingly, TMS does yield a possible semimetallic state with the appearing of new and softening vibrational modes at 96 GPa,[39] which resembles the case on hydrogen in phase IV upon compression to 278 GPa, indicated by Raman spectrum.[4] These theoretical and experimental results are encouraging for the experimental detection of the metallization in such materials because the resistance measurements on a similar aromatic hydrocarbon indeed reveal the metallic state at a much low pressure of 40 GPa than generally thought.[62] Further electrical transport measurements are expected on the studied material.

4. Conclusions

We perform high-pressure powder x-ray diffraction measurements on TMS at up to 31.1 GPa. Our results reveal the homogeneous process of phase transitions for TMS with compression to 31.1 GPa compared with the aforementioned work on Raman spectrum investigations of liquid TMS. A new phase possesses a space group of *Pnma* at 4.2 GPa , which is identified by the XRD patterns at pressure up to 31.1 GPa. After that, the material transforms into phase IV with the $P2_1/c$ symmetry and phase V with monoclinic $P2/m$ structure at the corresponding pressures of 9.9 GPa and 19.8 GPa respectively via a transitional phase in a pressure range of 6.5 GPa–8.6 GPa. These structural transitions suggest that they result from the changes in the inter- and intra-molecular bonding of this material. Interestingly, $P2_1/c$ structure of TMS has unique lattice parameters compared with those of the compounds containing relevant tetraheddral molecules, which makes TMS continue to crystallize but not realize decomposition nor amorphization upon compression. Additionally, the appearing of $P2/m$ space gronp in phase V offers a possibility to achieve the metallization in this material with further compression. Such structural information will encourage one to experimentally detect the metallization in such materials by other methods.

Acknowledgment

We thank Dr. Zhi-Qiang Chen for supporting the x-ray diraction measurements. Use of the National Synchrotron Light Source, Brookhaven National Laboratory, was supported by the U.S. Department of Energy, Office of Science, Office of Basic Energy Sciences, under Contract No. DE-AC02-98CH10886.

References

[1] Ginzburg V L 2004 *Rev. Mod. Phys.* **76** 981
[2] Ashcroft N W 1968 *Phys. Rev. Lett.* **21** 1748
[3] Richardson C F and Ashcroft N W 1997 *Phys. Rev. Lett.* **78** 118
[4] Howie R T, Guillaume C L, Scheler T, Goncharov A F and Gregoryanz E 2012 *Phys. Rev. Lett.* **108** 125501
[5] Zha C S, Liu Z and Hemley R J 2012 *Phys. Rev. Lett.* **108** 146402
[6] Loubeyre P, Occelli F and LeToullec R 2002 *Nature* **416** 613
[7] Ashcroft N W 2004 *Phys. Rev. Lett.* **92** 187002
[8] Drozdov A P, Eremets M I and Troyan I A 2014 arXiv: 1412.0460
[9] Feng J, Grochala W, Jaroń T, Hoffmamoto R, Bergara A and Ashcroft N W 2006 *Phys. Rev. Lett.* **96** 017006
[10] Pickard C J and Needs R J 2006 *Phys. Rev. Lett.* **97** 045504
[11] Yao Y, Tse J S, Ma Y and Tanaka K 2007 *Europhys. Lett.* **78** 37003
[12] Degtyareva O, Canales M M, Bergara A, Chen X J, Song Y, Struzhkin V V, Mao H K and Hemley R J 2007 *Phys. Rev. B* **76** 064123
[13] Chen X J, Wang J L, Struzhkin V V, Mao H K, Hemley R J and Lin H Q 2008 *Phys. Rev. Lett.* **101** 077002
[14] Chen X J, Struzhkin V V, Song Y, Goncharov A F, Ahart M, Liu Z X, Mao H K and Hemley R J 2008 *Proc. Natl. Acad. Sci. USA* **105** 20
[15] Eremets M I, Trojan I A, Medvedev S A, Tse J S and Yao Y 2008 *Science* **319** 1506
[16] Kim D Y Scheicher R H, Leb'egue S, Prasongkit J, Arnaud B, Alouani M and Ahuija R 2008 *Proc. Natl. Acad. Sci. USA* **105** 16454
[17] Martinez-Canales M, Oganov A R, Ma Y, Yan Y, Lyakhov A O and Bergara A 2009 *Phys. Rev. Lett.* **102** 087005
[18] Degtyareva O, Proctor J E, Guillaume C L, Gregoryanz E and Hanfland M 2009 *Solid State Commun.* **149** 1583
[19] Martinez-Canales M, Bergara A, Feng J and Grochala W 2006 *Chem. Solids* **67** 2095
[20] Li Z, Yu W and Jin C 2007 *Solid State Commun.* **143** 353
[21] Gao G Oganov A R, Bergara A, Martinez-Canales M, Cui T, Iitaka T, Ma Y and Zou G 2008 *Phys. Rev. Lett.* **101** 107002
[22] Zhang C, Chen X J, Li Y L, Struzhkin V V, Hemley R J, Mao H K, Zhang R Q and Lin H Q 2010 *J. Supercond. Nov. Magn.* **23** 717

[23] Zhang C, Chen X J, Li Y L, Struzhkin V V, Mao H K, Zhang R Q and Lin H Q 2010 *Europhys. Lett.* **90** 66006
[24] Tse J S, Yao Y and Ma Y 2007 *J. Phys.: Condens. Matter* **19** 425208
[25] Tse J S, Yao Y and Tanaka K 2007 *Phys. Rev. Lett.* **98** 117004
[26] Gonzalez-Morelos P, Hoffmann R and Ashcroft N W 2010 *Chem. Phys. Chem.* **11** 3105-8
[27] Gao G Oganov A R, Li P, Li Z, Wang H, Cui T, Ma Y, Bergara A, Lyakhov A O, Litaka T and Zou G 2010 *Proc. Natl. Acad. Sci. USA* **107** 1317
[28] Zaleski-Ejgierd P, Hoffmann R and Ashcroft N W 2011 *Phys. Rev. Lett.* **107** 037002
[29] Hanfland M Proctor J E, Guillaume C L, Degtyareva O and Gregoryan E 2011 *Phys. Rev. Lett.* **106** 095503
[30] Strobel T A, Goncharov A F, Seagle C T, Liu Z X and Somayazulu M 2011 *Phys. Rev. B* **83** 144102
[31] Rank D H and Bordner E R 1935 *J. Chem. Phys.* **3** 248
[32] Anderson T F 1936 *J. Chem. Phys.* **4** 161
[33] Silver S 1940 *J. Chem. Phys.* **8** 919
[34] Watari F 1978 *Spetrochimica Acta* **34A** 1239
[35] Shimizu K and Murata H J 1960 *Mol. Spectrosc.* **5** 44
[36] Young C W, Koehler J S and Mckinney D S 1947 *J. Am. Chem. Soc.* **69** 1410
[37] Wolf A K, Glinnemann J, Fink L, Alig E, Bolte M and Schmidt M U 2010 *Acta Cryst. B* **66** 229
[38] Gajda R and Katrusiak A 2008 *Cryst. Growth Des.* **8** 211
[39] Qin Z X, Zhang J B, Troyan I, Palasyuk T, Eremets M and Chen X J 2012 *J. Chem. Phys.* **136** 024503
[40] Qin Z X, Tang L Y, Liu J and Chen X J 2013 *Chin. Phys. C* **37** 098001
[41] Larson A C and Von-Dreele R B 1994 GSAS — General Strcture Analysis System. Report LAUR 86-748. Los Alamos National Laboratory, USA
[42] Murli C and Song Y 2009 *J. Phys. Chem. B* **113** 13509
[43] Hasebe T, Soda G and Chihara H 1975 *Proc. Jpn. Acad.* **51** 168
[44] Harada M, Atake T and Chihara H 1977 *J. Chem. Thermodyn.* **9** 523
[45] Zakharov L N, Antipin M Y, Struchkov Y T, Gusev A V, Gibbin A M and Zhernenkov N V 1968 *Kristallografiya* **31** 171
[46] Reuter H and Pawlak R 2000 *Z. Anorg. Allg. Chem.* **626** 925
[47] Reuter H and Pawlak R 2001 *Z. Kristallogr.* **216** 34
[48] Merz K and Driess M 2002 *Acta Cryst. C* **58** i101
[49] Köler J, Okudera H, Reuter D and Simon A 2005 *Z. Kristallogr.* **220** 523
[50] Wolf A K Glinnemann J, Schmidt M U, Tong J, Dinnebier R E, Simon A and Köhler J 2009 *Acta Cryst. B* **65** 342
[51] Lima-Jr J A, Freire P, Melo F, Lemos V, Mendes-Filho J and Pizani P 2008 *J. Raman Spectrosc.* **39** 1356
[52] Qin Z X, Zhang C, Tang L Y, Zhong G H, Lin H Q and Chen X J 2012 *Phys. Rev. B* **86** 184110
[53] Brand P and Sackmann H 1963 *Acta Crystallogr.* **16** 446
[54] Hearne G R, Pasternak M P and Taylor R D 1995 *Phys. Rev. B* **52** 9209
[55] Chen A L, Yu P Y and Pasternak M P 1991 *Phys. Rev. B* **44** 2883
[56] Pasternak M P, Taylor R D, Kruger M B, Jeanloz R, Itie J P and Polian A 1994 *Phys. Rev. Lett.* **72** 2733
[57] Hamaya N, Sato K, Usui-Watanabe K, Fuchizaki K, Fujii Y and Ohishi Y 1997 *Phys. Rev. Lett.* **79** 4597
[58] Pasternak M P and Taylor R D 1988 *Phys. Rev. B* **37** 8130
[59] Williamson W and Lee S A 1991 *Phys. Rev. B* **44** 9853
[60] Fujii Y, Kowaka M and Onodera A 1985 *J. Phys. C* **18** 789
[61] Qin Z X, Chen X J, Zhang C, Tang L Y, Zhong G H, Lin H Q, Meng Y and Mao H K 2013 *J. Chem. Phys.* **138** 024307
[62] Aust R B, Bentley W H and Drickamer H G 1964 *J. Chem. Phys.* **41** 1856
[63] Rietveld H M 1969 *J. Appl. Cryst.* **2** 65